Fuel 89 (2010) 2791–2801

Contents lists available at ScienceDirect

Fuel

journal homepage: www.elsevier.com/locate/fuel

# Dynamic modelling and analysis of post-combustion $CO_2$ chemical absorption process for coal-fired power plants

A. Lawal [a], M. Wang [a,*], P. Stephenson [b], G. Koumpouras [c], H. Yeung [a]

[a] Process Systems Engineering Group, School of Engineering, Cranfield University, Bedfordshire MK43 0AL, UK
[b] RWE npower, Windmill Park, Swindon SN5 6PB, UK
[c] Process Systems Enterprise Ltd., Hammersmith W6 7HA, UK

ARTICLE INFO

*Article history:*
Received 20 November 2009
Received in revised form 30 April 2010
Accepted 20 May 2010
Available online 2 June 2010

*Keywords:*
$CO_2$ capture
Post-combustion
Chemical absorption
Dynamic modelling
Coal-fired power plant

ABSTRACT

Post-combustion capture by chemical absorption using MEA solvent remains the only commercial technology for large scale $CO_2$ capture for coal-fired power plants. This paper presents a study of the dynamic responses of a post-combustion $CO_2$ capture plant by modelling and simulation. Such a plant consists mainly of the absorber (where $CO_2$ is chemically absorbed) and the regenerator (where the chemical solvent is regenerated). Model development and validation are described followed by dynamic analysis of the absorber and regenerator columns linked together with recycle. The gPROMS (Process Systems Enterprise Ltd.) advanced process modelling environment has been used to implement the proposed work. The study gives insights into the operation of the absorber–regenerator combination with possible disturbances arising from integrated operation with a power generation plant. It is shown that the performance of the absorber is more sensitive to the molar *L*/*G* ratio than the actual flow rates of the liquid solvent and flue gas. In addition, the importance of appropriate water balance in the absorber column is shown. A step change of the reboiler duty indicates a slow response. A case involving the combination of two fundamental $CO_2$ capture technologies (the partial oxyfuel mode in the furnace and the post-combustion solvent scrubbing) is studied. The flue gas composition was altered to mimic that observed with the combination. There was an initial sharp decrease in $CO_2$ absorption level which may not be observed in steady-state simulations.



## 1. Introduction

### 1.1. Background

Post-combustion capture by chemical absorption using MEA solvent remains the only commercial technology for large scale $CO_2$ capture for coal-fired power plants. It offers advantages over other $CO_2$ capture approaches as it is a suitable technology for retrofitting of existing power generation plants. It is also well suited for treating flue gas streams with low $CO_2$ partial pressures typical of coal-fired power plants.

Amongst stationary anthropogenic sources of $CO_2$ emissions, fossil-fuelled power plants release the largest amounts of $CO_2$. Coal-fired power plants release twice as much $CO_2$ per unit of electricity generated as their natural gas counterparts and are generally less efficient. However, these plants offer some advantages to operators due to the relatively high availability of coal compared to other fuels. Projections from the Energy Information Administration (EIA) suggest the continued use of coal especially in light of increasing electricity demand [1]. In addition, coal-fired power plants can be operated flexibly in response to changes in supply and demand [2] which provides great advantage to the operator.

### 1.2. Operation of the $CO_2$ chemical absorption plant and Grid Code requirements

Chemical absorption is a reactive absorption process and involves the combination of mass transfer and chemical reaction of $CO_2$ with a chemical solvent to form a weakly bonded intermediate compound which may be regenerated with the application of heat producing the original solvent and a $CO_2$ stream [3,4]. Monoethanolamine (MEA) being a primary amine reacts with $CO_2$ to produce carbamate via sets of liquid phase reactions [5,6].

Fig. 1 describes a typical chemical absorption plant. The facility consists of two main units – the absorber and regenerator columns which could be packed or tray columns. Flue gas from the power plant is contacted counter-currently with lean MEA solution in the absorber. MEA chemically absorbs $CO_2$ in the flue gas. This leaves a treated gas stream of much lower $CO_2$ content. The solvent solution (now Rich MEA) is regenerated in the regenerator column using steam derived from the power generation process. This

* Corresponding author. Tel.: +44 1234 754655; fax: +44 1234 754685.
*E-mail address:* meihong.wang@cranfield.ac.uk (M. Wang).

0016-2361/$ - see front matter © 2010 Elsevier Ltd. All rights reserved.
doi:10.1016/j.fuel.2010.05.030

**Nomenclature**

| | |
|---|---|
| $A$ | cross-sectional area ($m^2$) |
| $c_t$ | total molar concentration ($mol/m^3$) |
| $f$ | fugacity coefficient |
| $F_i$ | component mass flow rate (kg/s) |
| $F_H$ | enthalpy flow rate (J/s) |
| $H$ | heat flux ($J/m^2s$) |
| $h$ | specific enthalpy (J/mol) |
| $HL$ | heat loss to surroundings ($J/m^3$) |
| $L$ | length of column section (m) |
| $L/G$ | liquid to gas |
| $M$ | mass holdup ($kg/m^3$) |
| $MW$ | molecular weight (kg/mol) |
| $N$ | molar flux ($mol/m^2$ s) |
| $NAE$ | Number of axial elements |
| $nc$ | number of components |
| $R$ | universal gas constant (J/mol K) |
| $Sp$ | specific area ($m^2/m^3$) |
| $U$ | energy holdup ($J/m^3$) |
| $X$ | mass fraction |
| $x_i^M$ | molar fraction |
| $y$ | axial position |
| $z$ | Film position |

*Greek symbols*

| | |
|---|---|
| $\delta$ | film thickness (m) |
| $\lambda$ | thermal conductivity (W/m K) |
| $\mu$ | viscosity (Pa s) |
| $\omega$ | wetted area ratio |
| $\chi$ | diffusivity ($m^2/s$) |
| $\gamma$ | $CO_2$ loading (mol $CO_2$/mol MEA) |

*Subscripts*

| | |
|---|---|
| *abs* | absorption |
| *H* | enthalpy |
| *i* | component number |
| *Liq* | liquid |
| *Vap* | vapour |

*Superscripts*

| | |
|---|---|
| *Cond* | conduction |
| *Conv* | convection |
| *I* | interface |
| *L* | liquid |
| *Lb* | liquid bulk |
| *Lf* | liquid film |
| *M* | molar |
| *R* | reference |
| *V* | vapour |
| *Vb* | vapour bulk |
| *Vf* | vapour film |

steam is proposed to be extracted between the intermediate pressure and low pressure turbines. $CO_2$ from the top of the column is compressed and transported away while the lean (regenerated) MEA solution is returned to the absorber column completing the cycle.

System frequency in a Grid is determined by a balance in system demand and total power generation. When the demand rises above the power generated, the frequency drops and vice versa. The UK Grid Code demands relatively strict minimum requirements for primary frequency response in power generation. Power plants are required to have the capacity to increase their output by 10% over a 10-s period. Secondary response refers to the requirement of output increase between 30 s and 30 min [7]. One reason why subcritical power plants can meet the UK Grid requirements is that they have boiler drums and as such have a large amount of stored energy. Higher efficiency supercritical boilers do not have drums and therefore it may be harder for them to meet Grid requirements. There are therefore concerns that these supercritical plants may not be able to meet the primary response requirement of the UK Grid Code [7]. In such a situation, some benefits may accrue from addition of a post-combustion plant downstream the power plant as the steam supplied to the reboiler could be reduced to make more steam available for power generation thus aiding primary response. It is, therefore, important to understand the behaviour of the absorption process with such a reduction. Storage of rich amine solvent could enable this to be done without a drop in $CO_2$ capture levels [8].

In addition, with a likely increase in the proportion of renewable energy sources, coal-fired power plants with CCS may be forced to operate flexibly to support the intermittency of such renewable sources [8]. The flue gas supplied to the absorption process may therefore vary in flow rate or composition as the power plant operates in varying load conditions. It is therefore important to investigate the response of the capture plant to the power plant's load-following operation.

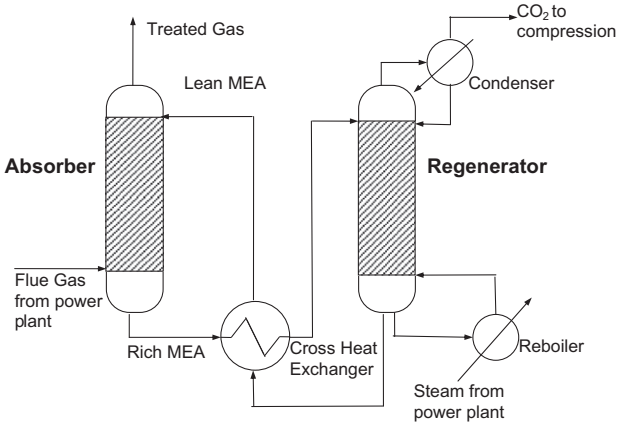


**Fig. 1.** Simplified process flow diagram of chemical absorption process for post-combustion capture from [4].

### 1.3. Novel contributions

This study investigates the operation of coal-fired power plants with post-combustion capture using dynamic modelling and simulation. Several authors have studied the reduction in the overall efficiency of the power generation process due to the large energy requirements of chemical absorption of $CO_2$ on a steady-state basis [5,9–11]. However, these studies thus assume that the power plant operates continuously at base-load conditions. Such studies cannot provide insight into plant performance during certain operations such as start-up, load variations and other disturbances. Accurate dynamic models are required to study this behaviour.

Kvamsdal et al. [12] and Lawal et al. [13] present the dynamic model development and simulation of the absorber only. Lawal et al. [13] also discuss different types of models used for modelling reactive absorption and the developments made in this regard.

Ziaii et al. [14] describe the dynamic model development and simulation of the regenerator only while Lawal et al. [15] extend this to the two stand-alone columns. Analysis on stand-alone columns may be inaccurate due to the inevitable coupling of the two columns linked with a recycle loop. This study presents dynamic modelling and simulation of the $CO_2$ chemical absorption plant that is the absorber and regenerator linked together with recycle. As a result the dynamic interaction between the absorber and regenerator could be studied more accurately through dynamic analysis.

### 1.4. Outline of the paper

Section 1 gives the background and motivation for this study. Section 2 describes the model development process for the rate-based models. The validation of the developed models is discussed in Section 3. In Section 4, four dynamic cases describe how disturbances affect the operation of the $CO_2$ chemical absorption plant.

(a) A system with poor water balance – this is a major control issue in chemical absorption plant [16,17].
(b) Increased flue gas flow rate to the absorber – this would occur with a shift from part-load power plant operation to a higher load. The case mimics a possible secondary frequency response scenario.
(c) A possible primary response scenario where there is reduced steam flow available for regeneration.
(d) An increased concentration of $CO_2$ in the flue gas from the power generation process. A partial $O_2$ fired coal power plant with post-combustion capture is discussed in [18]. Increased $O_2$ concentration in combustion air would increase $CO_2$ concentration in the resulting flue gas. This should reduce the demand on the capture plant to achieve desired $CO_2$ capture levels. This case shows what happens to the capture plant as the composition of the flue gas changes significantly.

## 2. Model development

This section describes development of the dynamic model of the $CO_2$ chemical absorption plant. Common to both absorber and regenerator columns is the packed column section. These two columns were modelled based on the gPROMS Advanced Model Library for Gas–Liquid Contactors (AML:GLC). Two phenomena determine the rates of $CO_2$ absorption and solvent regeneration – mass transfer and chemical reaction. Mass transfer rates were modelled based on the two-film theory (Fig. 2) using the Maxwell–Stefan formulation hence the models are referred to as "rate-based models". Heat and mass transfer resistances are modelled in the liquid and vapour films. Mass transfer coefficients in the liquid and vapour films were determined by correlations given by Onda et al. [19]. The diffusivity ($\chi$) of $CO_2$ in the liquid phase was based on expressions provided by Vaidya and Mahajani [20]. The diffusivity ($\chi$) of $CO_2$ and other components in the vapour phase was estimated using the Fuller's equation [21]. Expressions for the heat of absorption were obtained from the literature [22].

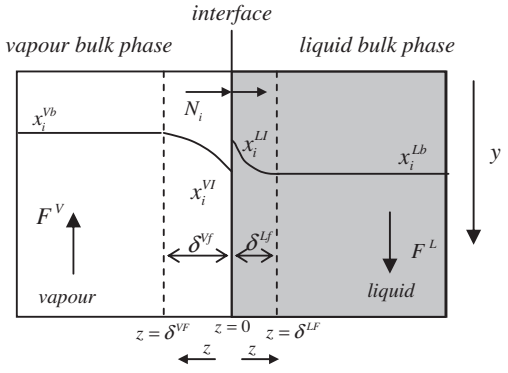


**Fig. 2.** Liquid and vapour bulks, films and interface.

The regenerator model consists of the Gas–Liquid Contactor model (for the packed column section) linked with two flash drum models which represent the condenser and reboiler of the unit.

In the absorber, it is assumed that there is no heat lost to the surroundings. Due to its relatively higher operating temperature, the regenerator energy balance includes a heat loss term. Heat loss was assumed constant along the height of the column. The total heat loss from the column was estimated using relations given by Dugas [23].

### 2.1. Model assumptions

The following assumptions were used in developing this dynamic model:

(1) All reactions are assumed to attain equilibrium.
(2) Plug flow regime and linear pressure drop along the column.
(3) Phase equilibrium at interface between liquid and vapour films.
(4) Negligible holdup in the vapour bulk.
(5) Negligible solvent degradation.
(6) Negligible heat loss in the absorber column due to relatively lower operating temperatures.
(7) Chemical reactions are assumed to reach equilibrium in the condenser and reboiler.

### 2.2. Model equations

More details of the absorber dynamic model are described in [13] while regenerator dynamic model is further described in [15]. In the packed column section, the main models include the vapour and liquid bulk models, the vapour and liquid film models and the interface (Fig. 2). The main equations are listed for the convenience of readers.

#### 2.2.1. Liquid bulk model

$$\text{Mass Balance}: \quad \frac{dM_i}{dt} = \frac{-1}{L \cdot A}\frac{\partial F_i^L}{\partial y} + N_i \cdot Sp \cdot MW_i \cdot \omega \tag{1}$$

The change in component mass holdup, $M_i$, with respect to time is determined by the differential change of the component mass flow along the axis of the column $\frac{\partial F_i^L}{\partial y}$ and the estimated component molar fluxes to and from the liquid bulk $N_i$

$$\text{Energy Balance}: \quad \frac{dU}{dt} = \frac{-1}{L \cdot A}\frac{\partial F_H^L}{\partial y} + Sp \cdot \omega \cdot \left(H_{liq}^{cond} + H_{liq}^{conv} + H_{abs}\right) + HL \tag{2}$$

The change in energy holdup with respect to time, $\frac{dU}{dt}$, is determined by the differential change of 'energy flow' along the axis of the column, $\frac{\partial F_H^L}{\partial y}$ and the liquid heat fluxes at the liquid film-liquid bulk interface due to conduction, $H_{liq}^{cond}$, convection, $H_{liq}^{conv}$ as well as the heat flux due to chemical absorption of $CO_2$, $H_{abs}$

$$\text{Heat Loss } (HL) = \frac{342.88 \cdot (T_{regen\_bottom} - T_{ambient})}{L \cdot A \cdot NAE} \tag{3}$$

The Heat Loss ($HL$) in the regenerator is calculated based on the temperature difference between the regenerator bottoms temperature ($T_{regen\_bottom}$) and the ambient temperature ($T_{ambient}$). It is calculated per unit volume and distributed evenly along the axial length of the column

$$\text{Heat of absorption (or desorption)}: \quad H_{abs} = N_{CO_2} \cdot h_{abs} \tag{4}$$

$$h_{abs} = R \cdot \left( -14281 - \left( \frac{1092554 \cdot \gamma^2}{T} \right) - \left( \frac{6800882 \cdot \gamma}{T} \right) + 32670.01 \cdot \gamma \right) \tag{5}$$

The specific heat of absorption, $h_{abs}$, was estimated based on the temperature, $T$, and the $CO_2$ loading of the solvent, $\gamma$. $R$ is the universal gas constant.

*2.2.2. Vapour bulk model*

$$\text{Mass Balance}: \quad 0 = \frac{-1}{L \cdot A} \frac{\partial F_i^V}{\partial y} - N_i \cdot Sp \cdot MW_i \cdot \omega \tag{6}$$

$$\text{Energy Balance}: \quad 0 = \frac{-1}{L \cdot A} \frac{\partial F_H^V}{\partial y} + Sp \cdot \omega \cdot \left( H_{vap}^{cond} + H_{vap}^{conv} \right) \tag{7}$$

In the vapour bulk, it is assumed that the accumulation of mass and energy holdups are negligible. This was assumed because the residence time of the vapour phase in the absorption system is relatively small compared to that of the circulated liquid phase solvent. The composition and temperature would change along the axial direction of the column, however. Chemical absorption of $CO_2$ is assumed to take place through liquid phase reactions; therefore, the heat of absorption is accounted for only in the liquid bulk energy balance. In addition, the heat losses to the surroundings are fully accounted for in the liquid phase so this term is not repeated in the vapour bulk energy balance.

*2.2.3. Vapour and liquid film models*

Maxwell–Stefan Formulation:

$$\frac{1}{\delta} \frac{\partial x_i^M}{\partial z} = \frac{1}{c_t} \sum_{k=1}^{nc} \left( \frac{x_i^M N_k - x_k^M N_i}{\chi_{i,k}} \frac{\mu^R}{\mu} \frac{T}{298.15} \right), \; k \neq i \tag{8}$$

Mass transfer rates are determined using the Maxwell–Stefan formulation. Corrections are made to the formulation for different viscosities, $\mu$, (relative to the reference viscosity $\mu^R$) as well as for different temperatures ($T$) relative to the reference temperature of 298.15 K.

In the mass balance, it is assumed that there is no accumulation of mass in the film. The energy balance is given in Eq. (9). For a film of thickness, $\delta$,

$$\frac{1}{\delta} \frac{\partial(\lambda G_T)}{\partial z} - \frac{1}{\delta} \frac{\partial H_{flux}}{\partial z} = 0 \tag{9}$$

where $\lambda$ is the thermal conductivity of the fluid and the temperature gradient, $G_T$, is defined as

$$G_T = \frac{1}{\delta} \frac{\partial T}{\partial z} \tag{10}$$

The heat per surface flux, $H_{flux}$ across the film thickness is defined as

$$H_{flux} = \sum_{i=1}^{nc} N_i h_i^M \tag{11}$$

where $h_i^M$ is the specific molar enthalpy and $N_i$ is the component molar flux.

At the film–bulk interface the heat fluxes due to conduction and convection used in Eqs. (2) and (7) are estimated as follows:

$$H^{cond} = \frac{-\lambda}{\delta} \frac{\partial T|_{z=1}}{\partial z} \tag{12}$$

$$H^{conv} = H_{flux}|_{z=1} = \sum_{i=1}^{nc} N_i|_{z=1} h_i^M \Big|_{z=1} \tag{13}$$

*2.2.4. Interface model*

$$f_i^L \cdot x_i^{M,L} = f_i^V \cdot x_i^{M,V} \tag{14}$$

Phase equilibrium between liquid and vapour phases is assumed at the interface. The equilibrium molar compositions of the components in the vapour and liquid phases, $x_i^M$, are estimated based on the vapour and liquid fugacity coefficients, $f_i$.

*2.2.5. Physical property estimation*

Physical property estimations for viscosities, enthalpies and densities were determined using a physical property package, Multiflash while the fugacity coefficients and flash calculations in the reboiler and condenser were determined using the Electrolyte Non-random-two-liquid (NRTL) model in Aspen Properties and accessed through the CAPE-OPEN Thermo interface.

*2.3. Controllers for the process*

Control schemes are illustrated in Fig. 3 and listed in Table 1. PI controllers are used for temperature control of the regenerator column. The temperatures of the top and bottom of the regenerator are manipulated using the condenser and reboiler heat duties. The temperature of the regenerated solvent determines its $CO_2$ loading and thus affects its absorption capacity. Therefore, the temperature of the solvent from the regenerator bottoms must be maintained at desired levels.

The reboiler level was controlled using a P controller by manipulating the reboiler bottoms flow rate.

Water balance is achieved by controlling the water mass fraction in the lean solvent with the water makeup flow rate used as manipulated variable. A typical composition of the Lean MEA stream consists of 30.48wt% MEA, 6.18 wt% $CO_2$ which leaves a 63.34 wt% $H_2O$. The set point for the mass fraction of water in the lean solvent was therefore set as 0.6334.

The percentage of $CO_2$ captured is measured by comparing the $CO_2$ mass flows in the flue gas stream to the absorber and the flue gas stream from the top of the absorber. This value is then controlled by manipulating the lean MEA solvent flow rate.

The cross heat exchanger was sized to yield the reported regenerator feed temperature and a temperature approach of over 15 °C. The cooler upstream the Lean MEA tank is specified to have a constant outlet temperature. The pressure of the partial condenser is controlled by a non-return valve as shown in Fig. 3 to maintain the regenerator column operating pressure. The Rich MEA from absorber pump is specified to deliver the differential pressure between the absorber and regenerator including the pressure drops of the equipment in between.

*2.4. Model topology*

Assumptions for model topology

(1) No water wash section in the absorber. The water wash section would help control the temperature of the flue gas leaving the absorber which is required for adequate water balance. However, the pilot plant study used to validate the model developed did not include a water wash section in the absorber. In the study, it was assumed that a similar topology as the pilot plant was maintained.
(2) To control water balance in the absorber, an idealistic case was assumed where a controller maintained the water composition in the lean solvent being circulated. The lean amine solvent from the regenerator is fed into the Lean MEA tank where water is made up before being pumped to the absorber. This approach would not be applicable in a real plant

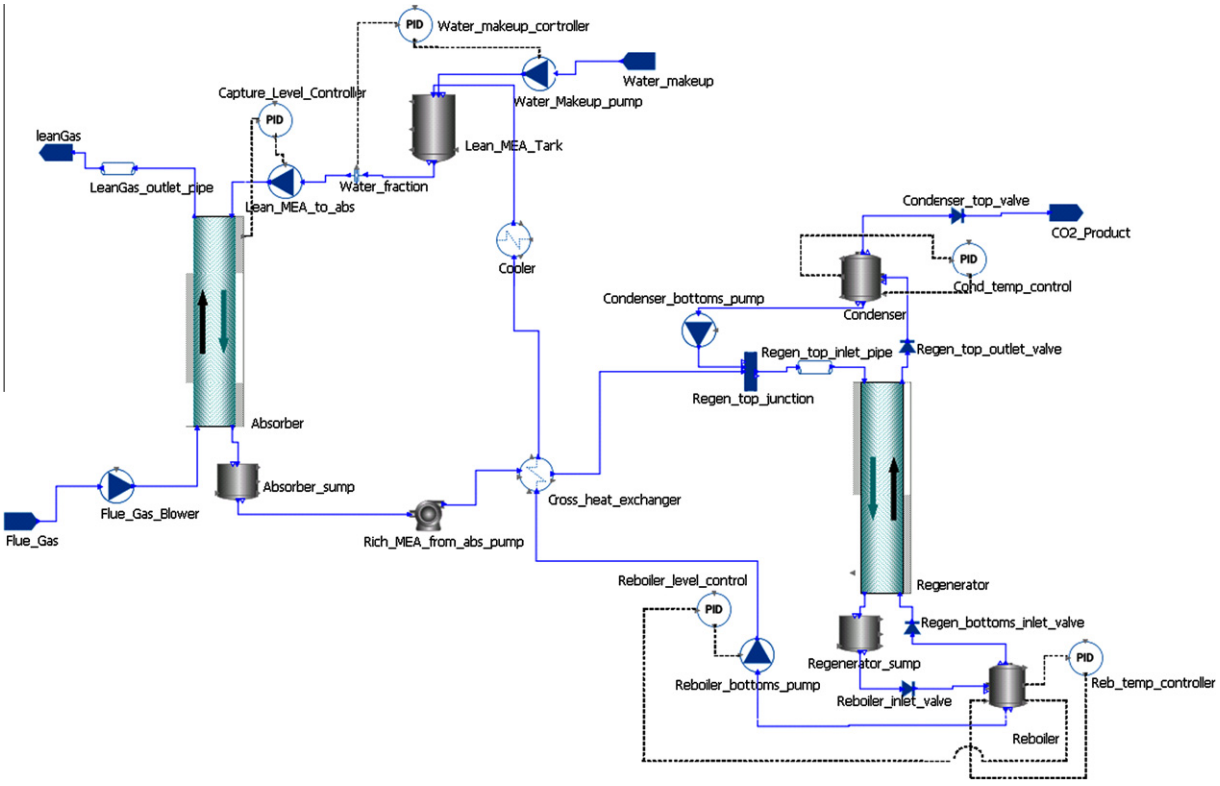


**Fig. 3.** Model topology in gPROMS.

**Table 1**
Process controllers.

| | Controlled variable | Manipulated variable | Set point |
|---|---|---|---|
| Condenser temperature controller | Condenser temperature | Condenser heat duty | 320 K |
| Reboiler temperature controller | Reboiler temperature | Reboiler heat duty | 387 K |
| Reboiler level controller | Reboiler level | Reboiler bottoms flow rate | 0.50 |
| Water makeup controller | Water mass fraction in lean solvent | Water makeup flow | 0.6334 |
| Capture level controller | $CO_2$ capture level in absorber | Lean MEA solvent flow | 97% |

but was assumed for simplification. The water balance would likely be controlled by the temperature of the gas leaving the absorber.

(3) The absorber and regenerator sumps are modelled as simple tanks through which the bottom products flow as shown in Fig. 3.

## 3. Model validation

The steady-state validation of the chemical absorption plant model was carried out using data from the Separations Research Program at the University of Texas at Austin [23]. Dynamic validation of the model could not be carried out due to the lack of available plant data. The absorber and regenerator columns of the pilot plant are both packed columns with diameters of 0.427 m and total packing height of 6.1 m. Each column consists of two 3.05 m packed bed sections with a collector plate and redistributor between the beds.

Out of the 48 experimental cases carried out in the research program, two cases (Cases 32 and 47) were selected for steady-state validation purposes. These two cases were selected because of their relatively high and low liquid to gas ($L/G$) molar flow ratios for the absorber respectively. This further implies relatively high and low circulation rates of solvent as well as high and low capture levels respectively. In addition, the regenerator is operated at a relatively high absolute pressure of 1.6 bar in Case 32 while its operating pressure in Case 47 is 0.68 bar (absolute). Table 2 shows the process conditions for the lean and rich MEA and flue gas streams while Table 3 shows some absorber column and packing specifications. It should be noted that the compositions (mass fractions) of the various streams were estimated based on the available information. The capture level controller was the only controller described in Section 2.3 that was not active for the validation results presented.

Simulation results were validated using the temperature profile of the absorber column measured in the pilot plant [23]. In addition the measured $CO_2$ loading of the amine solvent taken at different positions was compared with values obtained from simulation.

### 3.1. Validation results of stand-alone columns

Figs. 4 and 5 show the validation results for the stand-alone column based on the temperature profile measured in the pilot plant for the two selected cases. Feed conditions to the absorber were inputted from the information available in [23] there was limited information available for the feed conditions to the regenerator. Therefore, for the stand-alone regenerator, the feed conditions were obtained from the rich solvent conditions estimated by the absorber model.

In general, the stand-alone models predict the general shape of the column temperature profiles. The deviations appear higher in the regenerator profile. This may be because (as explained earlier) any inaccuracies in the absorber model results would be propagated to the regenerator simulation.

**Table 2**
Process conditions for Cases 32 and 47.

| Stream ID | Case 32 | | | Case47 | | |
|---|---|---|---|---|---|---|
| | Flue gas | Lean MEA to absorber | Rich MEA from absorber | Flue gas | Lean MEA to absorber | Rich MEA from absorber |
| Temperature (K) | 320 | 314 | 358 | 332 | 313 | 356 |
| Total flow (kg/s) | 0.130 | 0.720 | 0.745 | 0.158 | 0.642 | 0.746 |
| *Mass fractions* | | | | | | |
| $H_2O$ | 0.0148 | 0.6334 | 0.6122 | 0.0193 | 0.6334 | 0.6085 |
| $CO_2$ | 0.252 | 0.0618 | | 0.2415 | 0.0618 | 0.0966 |
| MEA | 0 | 0.3048 | 0.2901 | 0 | 0.3048 | 0.2943 |
| $N_2$ | 0.7332 | 0 | 0.0006 | 0.7392 | 0 | 0.0006 |
| *L*/*G* ratio | | 6.5 | | | 4.6 | |

**Table 3**
Equipment specifications.

| Description | Value |
|---|---|
| Column internal diameter (m) | 0.427 |
| Height of packing (m) | 6.1 |
| Nominal packing size (m) | 0.0381 |
| Packing specific area (absorber) ($m^2/m^3$) | 145 |
| Packing specific area (regenerator) ($m^2/m^3$) | 420 |
| Cross heat exchanger heat transfer area ($m^2$) | 7 |
| Reboiler volume ($m^3$) | 1 |
| Condenser volume ($m^3$) | 2 |

### 3.2. Validation results of integrated model

Fig. 6 shows the validation results for the absorber and regenerator columns when they are linked together with recycle as shown in Fig. 3. The process conditions used are those of Case 32. The results show a different prediction of the temperature profile in the integrated model especially in the regenerator because of the limitations discussed in Section 3.1. In general, the integrated model gives a better prediction of the observed temperature profile. This is expected as the pilot plant consists of columns linked together with recycle and not stand-alone structure.

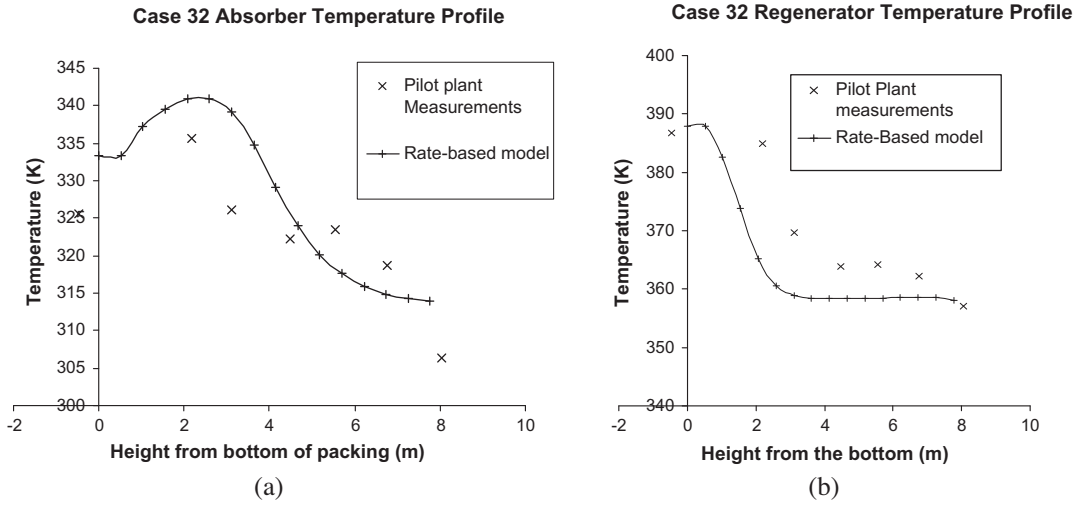


**Fig. 4.** (a) Absorber and (b) regenerator temperature profile of columns for Case 32 (stand-alone).

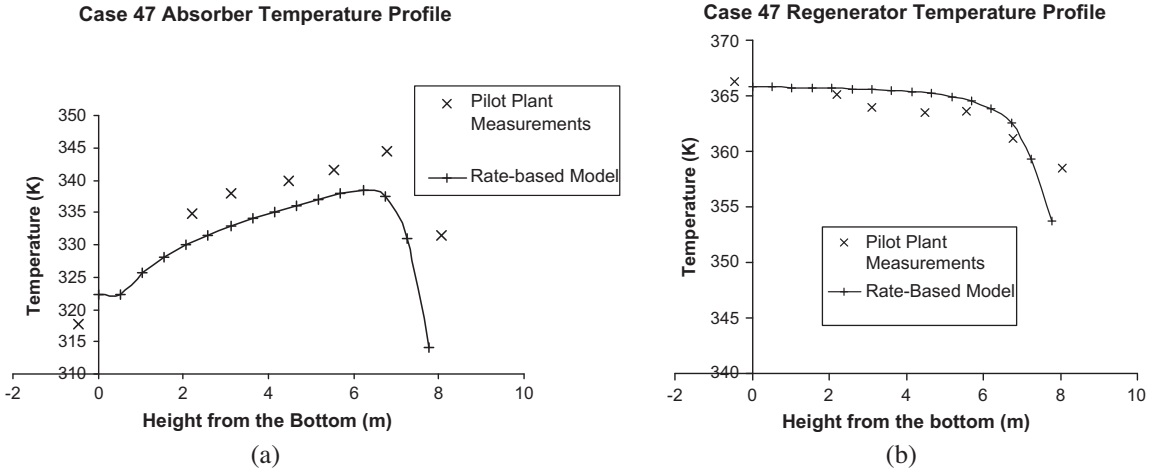


**Fig. 5.** (a) Absorber and (b) regenerator temperature profile for Case 47 (stand-alone).

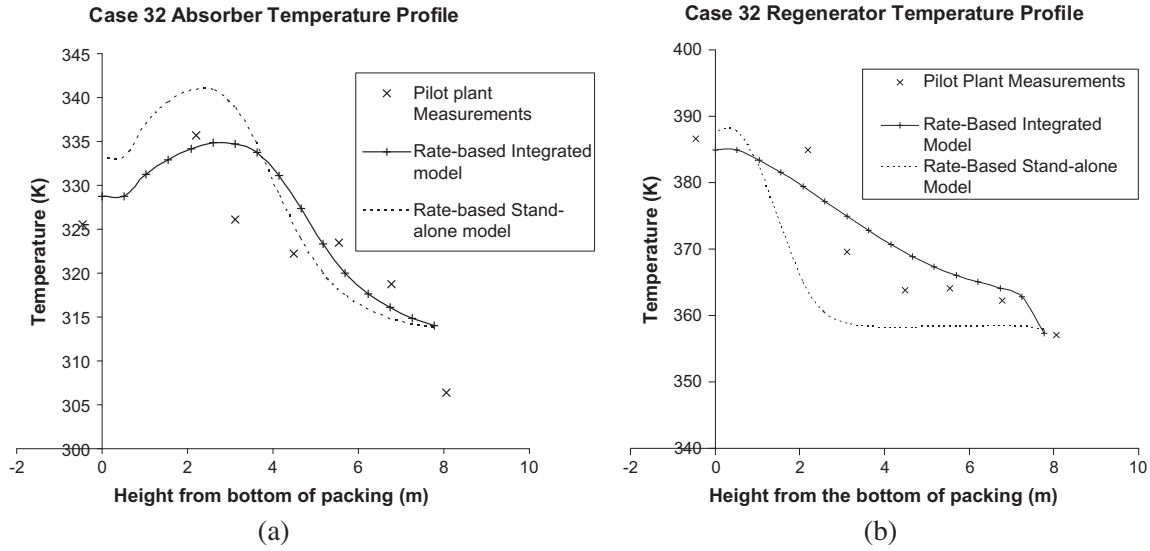


**Fig. 6.** (a) Absorber and (b) regenerator temperature profile of columns for Case 32 (integrated).

## 4. Dynamic analysis

The dynamic cases introduced in Section 1.4 are discussed further here.

### 4.1. Switching off water balance control

It was important to ensure that water balance is maintained in the process because an imbalance would introduce disturbances to the system. Kvamsdal et al. explained that the level of water saturation of the flue gas stream to the absorber and the temperature at which the treated gas stream from the top of the absorber column are key factors in determining the water balance in the system [16,17]. The temperature in the upper section of the absorber would increase with the exothermic absorption of $CO_2$ and condensation of water vapour while the temperature in the lower sections would decrease due to evaporation of water from the solvent. The combination of these phenomena would result in a tempera-

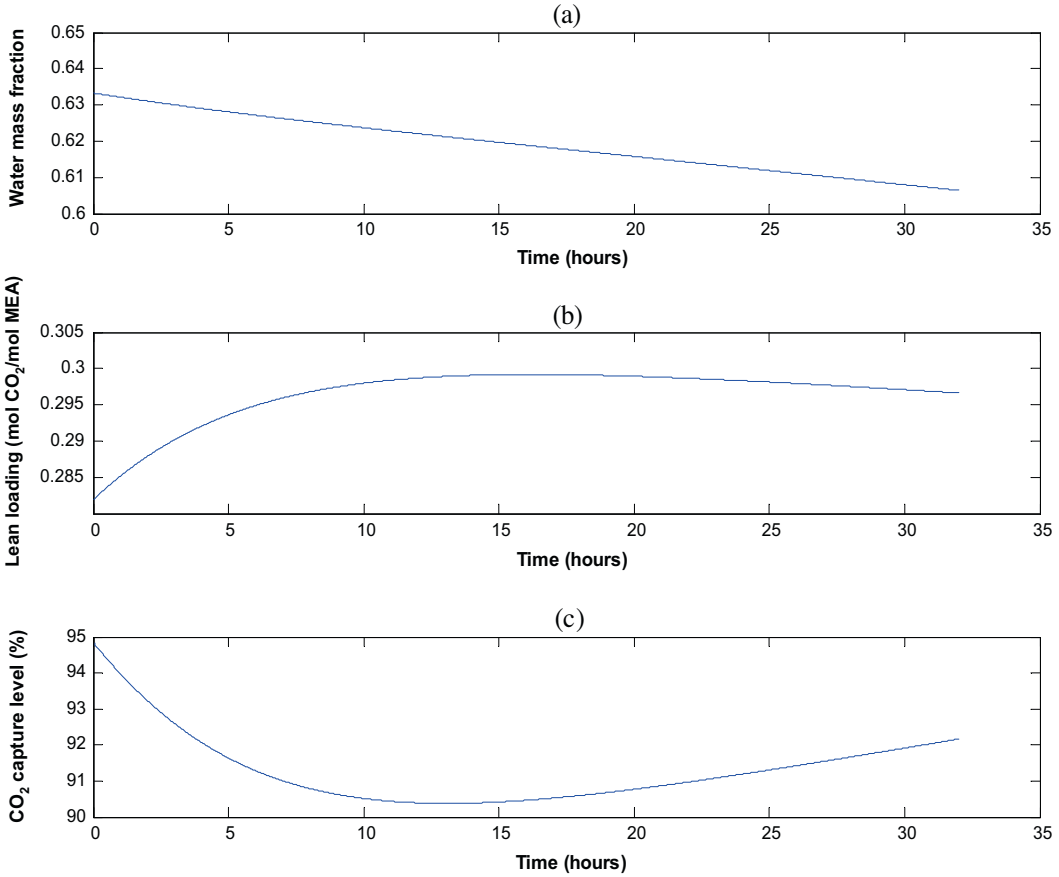


**Fig. 7.** Effects of poor water balance in $CO_2$ absorption process.

ture bulge [16,17]. The balance of evaporation and condensation would result in a net loss or gain of water vapour composition in the lean gas leaving the absorber.

Fig. 7 illustrates some of the effects the phenomenon could have. All the controllers in Section 2.3 were active except the water balance and capture level controllers. The same conditions for Case 32 were maintained for the integrated model as described in Section 3.2. Without any disturbances introduced, the $CO_2$ capture level varies significantly (Fig. 7c). This occurs because there is a net water loss (via evaporation) in the absorber column. As water was lost within the capture system through lean gas stream, the water mass fraction in the lean solvent reduces fairly steadily (Fig. 7a), the effect was an initial increase in the $CO_2$ loading of the lean solvent (Fig. 7b). A maximum loading is reached followed by a subsequent reduction with a resulting increase in $CO_2$ capture levels (Fig. 7c). This process could lead to severe operational problems such as corrosion if the concentrations of MEA and $CO_2$ in the solvent increase significantly.

### 4.2. Increasing flue gas flow rate to the absorber

This case simulates the effect of an increase in power plant output over a period of 10 min. It is assumed that this leads to a corresponding increase in flow rate of flue gas to the absorber and its composition is maintained. The process was simulated with the base-load conditions (Case 32) for 2 h and a 10% increase in flue gas flow rate was carried out over a period of 10 min after which the simulation was left to run for just less than 8 h. In both cases, all the controllers described in Section 2.3 were active except the capture level controller. In Case 1, the solvent circulation rate was kept constant while in Case 2, the circulation rate was correspondingly increased to maintain the molar $L/G$ ratio (Fig. 8).

Fig. 9 shows a decrease in $CO_2$ absorption levels at the onset of the disturbance for Case 1 and virtually the same capture level maintained for Case 2 after a slight drop. This is however at the cost of increased heat requirement for capture (Fig. 10). The heat required to capture a kg of $CO_2$ in Case 1 drops because the lean solvent had the capacity to capture more $CO_2$ at the same circulation rate. This is shown in Fig. 11. The difference between the $CO_2$ loading of the rich and lean MEA solvent streams flowing from and to the absorber respectively is estimated and plotted for the two cases. In Case 1, the solvent is in contact with significantly more $CO_2$ in the flue gas and thus absorbs more $CO_2$ yielding higher Rich MEA $CO_2$ loading. As the lean $CO_2$ loading is roughly maintained due to the constant reboiler temperature, more $CO_2$ is produced in the top $CO_2$ product. With a constant solvent circulation rate, the reboiler duty required to heat the solvent to the required set point of 387 K does not increase significantly. Thus the heat duty requirement for Case 1 reduces significantly. The heat duty requirement for capture for Case 2 is higher than that of Case 1

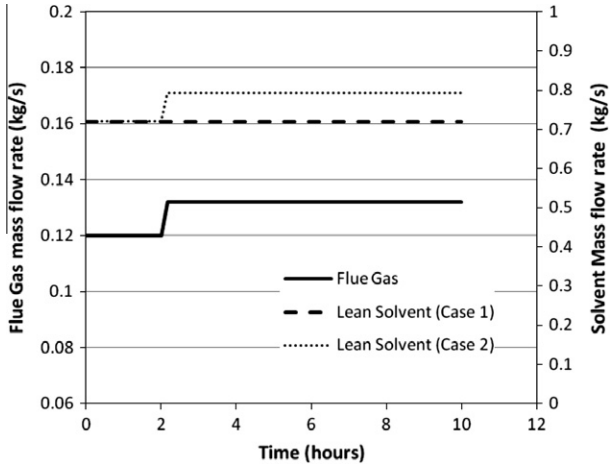


**Fig. 8.** Flue gas and lean MEA flow rate while increasing power plant load.

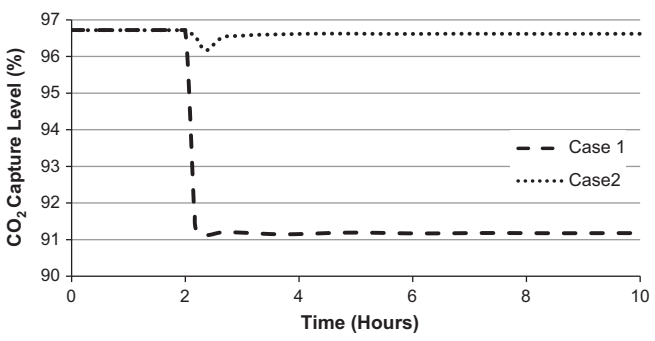


**Fig. 9.** $CO_2$ capture level with increasing power plant load (Case1 and Case 2).

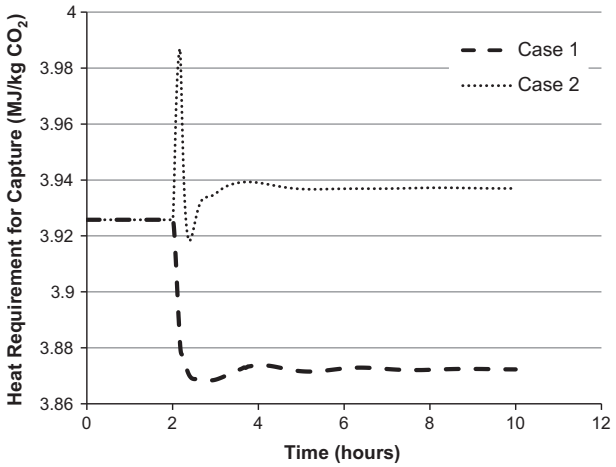


**Fig. 10.** Heat requirement with increasing power plant load (Case1 and Case2).

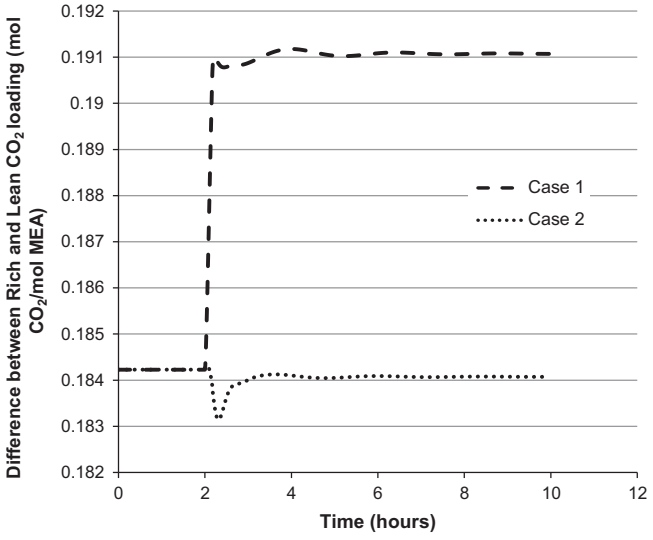


**Fig. 11.** Difference between rich and lean $CO_2$ loading for the absorber with increasing power plant load (Case1 and Case2).

but is maintained at almost the same level as before the disturbance (Fig. 10). The oscillations observed are due to controller action.

### 4.3. Reducing reboiler heat duty

This case investigates the effect of a decrease in reboiler heat duty. This required heat duty for regeneration is supplied from the power generation process. Storage of rich amine solvent from the absorber could enable this to be done without a drop in $CO_2$ capture levels. This scenario explores the effect of a drop in reboiler duty. Base conditions were maintained for a period of 2 h. A 10% reduction in reboiler duty was implemented over 10 s (Fig. 12). Conditions were maintained for just less than 8 h. All the controllers described in Section 2.3 were active except the capture level and reboiler temperature controllers.

A significant increase in $CO_2$ loading in the lean solvent is observed (Fig. 13) resulting from reduced reboiler temperatures. This also had a significant effect on the $CO_2$ capture levels in the absorber column (Fig. 14).

Since the change is carried out over a relatively short period of time, a time constant was estimated. The time constant estimated for the process was 3420 s or 57 min. It should be noted that the holdup of solvent in the absorber and regenerator sumps, the lean MEA storage tank as well as the reboiler would contribute to such a big time constant. The two sumps had a holdup of about 3 min each as well as the reboiler had a holdup of about 3 min. The lean MEA storage tank had a holdup of about 23 min. It also should be noted that in this model, transport delay has not been accounted for.

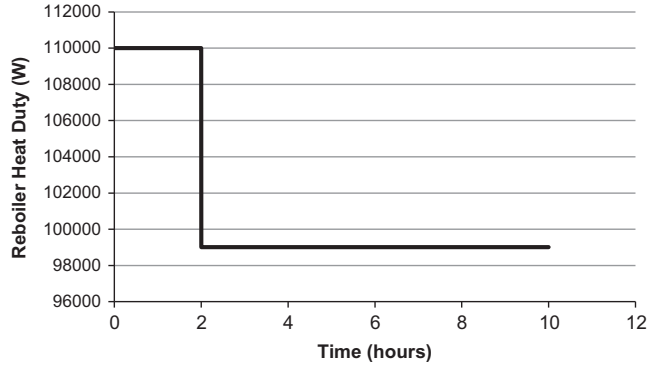


**Fig. 12.** Reducing reboiler heat duty.

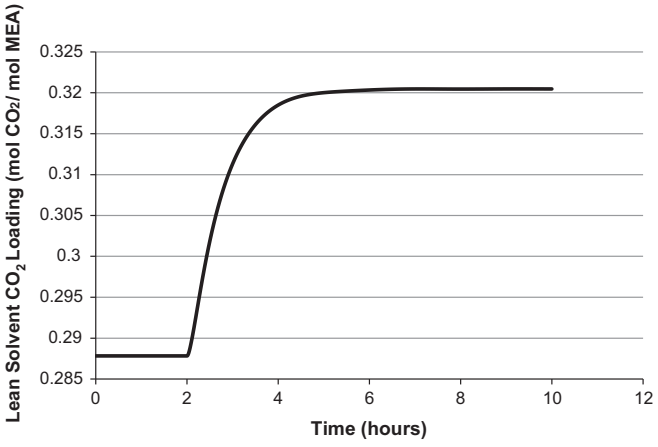


**Fig. 13.** $CO_2$ loading change with reduction in reboiler duty.

### 4.4. Increasing $CO_2$ concentration of flue gas to the absorber column

This case investigates the effect of increasing $CO_2$ concentration in the flue gas to the absorber. Some studies show that there could be benefits in a combination of two fundamental $CO_2$ capture technologies (the partial oxyfuel mode in the furnace and the post-combustion solvent scrubbing) [18]. Using partial oxyfuel mode, coal is burnt in a 50 vol% $O_2$ stream (rather than 21 vol% $O_2$ in the air), a flue gas of just less than 50 wt% $CO_2$ composition is produced. The change in composition of flue gas to the absorber as this

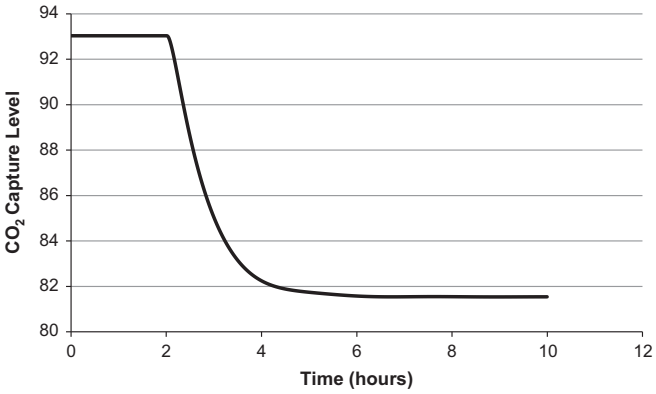


**Fig. 14.** $CO_2$ capture level with reduction in reboiler duty.

**Table 4**
New composition of flue gas with increasing $CO_2$ flue gas concentration.

| | Mass fractions | |
|---|---|---|
| | 100% air | 60% air |
| Water | 0.0148 | 0.0148 |
| Carbon dioxide | 0.2520 | 0.5751 |
| Nitrogen | 0.7332 | 0.4101 |
| Total mass flow (kg/s) | 0.1200 | 0.0526 |

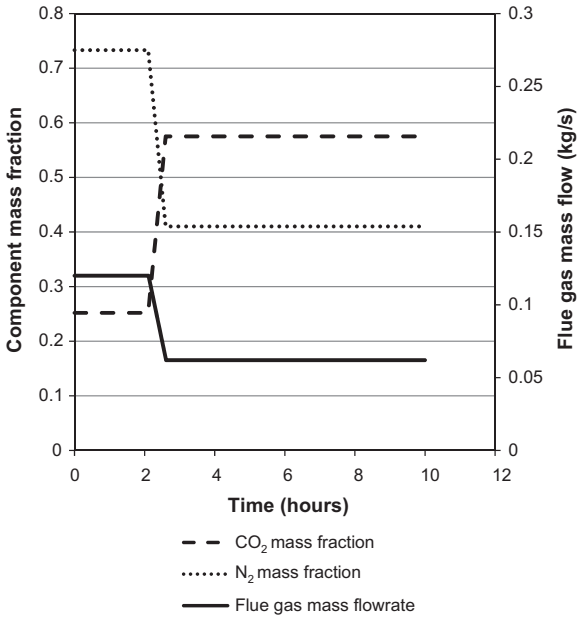


**Fig. 15.** Flue gas composition and mass flow with increasing $CO_2$ flue gas concentration.

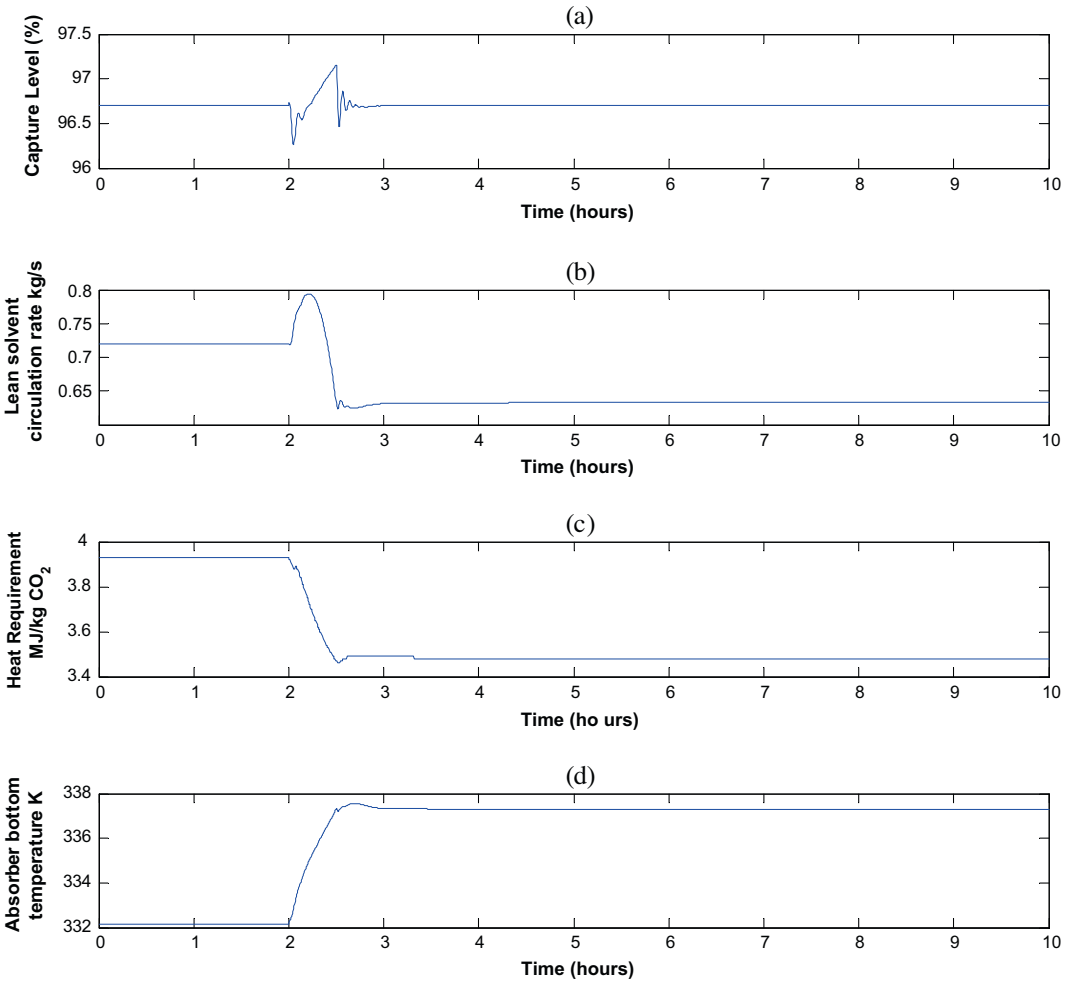


**Fig. 16.** Effects of increasing $CO_2$ flue gas concentration.

occurs is shown in Table 4. This should reduce the demand on the post-combustion capture plant to achieve desired $CO_2$ capture levels. The $CO_2$ mass flow to the absorber was kept constant while the total mass flow rate of the flue gas was correspondingly reduced (Fig. 15). Fig. 15 also shows the change in flue gas composition as this happens. The composition of water vapour is assumed constant as it is assumed there is a dryer upstream the capture plant that dries the flue gas stream to a constant water composition. These changes were assumed to be carried out over a period of 30 min. Conditions were maintained for about 7.5 h. All the control schemes discussed in Section 2.3 are active.

Fig. 16a shows the variation in $CO_2$ capture level with the capture level controller active. An initial drop in capture level is observed at the onset of the disturbance which is due to the increase in temperature (as seen in Fig. 16d). As a result, the lean MEA solvent circulation rate is first increased to compensate for this before it reduces to a steady-state value below the original. Less solvent (Fig. 16b) is needed to capture $CO_2$ because its concentration in the flue gas stream is significantly higher (Fig. 15). As the solvent circulation rate reduces, the heat duty requirement for capture also reduces (Fig. 16c).

## 5. Conclusions

This paper presents a study of $CO_2$ capture using chemical absorption based on the dynamic modelling of the absorber and regenerator columns linked together. Validation results show that the model predicts the absorber and regenerator temperature profiles and $CO_2$ loadings fairly well. It is shown that water balance in the absorption process is very important. Dynamic analyses show that the absorber performance is more sensitive to the molar $L/G$ ratio than the actual flow rates of the solvent and flue gas. The performance of the regenerator is affected by the reboiler duty and a time constant for the system was estimated as 57 min. It should be noted that the storage tanks and column sumps would contribute to this time constant. Some effects of increasing $CO_2$ flue gas concentration observed in the dynamic simulations such as an initial drop in capture levels may not be observed with steady-state simulations.

## Acknowledgements

This work is partly funded by RWE npower and its support is greatly appreciated. The technical support from Process Systems Enterprise (PSE) Ltd., UK is also appreciated.

## References

[1] Energy Information Administration (EIA). International Energy Annual; 2006. <www.eia.doe.gov/iea> [accessed February 2010].
[2] Chalmers H, Gibbins J. Initial evaluation of the impact of post-combustion capture of carbon dioxide on supercritical pulverised coal power plant part load performance. Fuel 2007;86(14):2109–23.
[3] IEA GHG. The capture of carbon dioxide from fossil fuel fired power stations. IEA GHG/SR2; 1993.

[4] IPCC. IPCC special report on carbon dioxide capture and storage. <www1.ipcc.ch/ipccreports/srccs.htm> [accessed September 2009]; 2005.
[5] Davidson R. Post-combustion carbon capture from coal fired plants – solvent scrubbing. Report CCC/125. IEA Clean Coal Centre www.iea-coal.org.uk; 2007.
[6] Kucka L, Müller I, Kenig EY, Górak A. On the modelling and simulation of sour gas absorption by aqueous amine solutions. Chem Eng Sci 2003;58(16):3571–8.
[7] EON UK. Supercritical coal fired plant requirements and the Grid Code. <www.nationalgrid.com/NR/rdonlyres/E3196A90-C091-463B-9113-440126B02A5E/25336/pp08_26_SuperCriticalcoalfiredplant.pdf> [accessed September 2009]; 2008.
[8] Haines MR, Davison JE. Designing carbon capture power plants to assist in meeting peak power demand. In: 9th International Conference on Greenhouse Gas Control Technologies; 16–20 November 2008. Washington (DC): Energy Procedia; 2008.
[9] Abu-Zahra MRM, Schneiders LHJ, Niederer JPM, Feron PHM, Versteeg GF. $CO_2$ capture from power plants: Part I. A parametric study of the technical performance based on monoethanolamine. International Journal of Greenhouse Gas Control 2007;1(1):37–46.
[10] Aroonwilas A, Chakma A, Tontiwachwuthikul P, Veawab A. Mathematical modelling of mass-transfer and hydrodynamics in $CO_2$ absorbers packed with structured packings. Chem Eng Sci 2003;58(17):4037–53.
[11] Davison J. Performance and costs of power plants with capture and storage of $CO_2$. Energy 2007;32(7):1163–76.
[12] Kvamsdal HM, Jakobsen JP, Hoff KA. Dynamic modelling and simulation of a $CO_2$ absorber column for post-combustion $CO_2$ capture. Chem Eng Process: Process Intensif 2009;48(1):135–44.
[13] Lawal A, Wang M, Stephenson P, Yeung H. Dynamic modelling and simulation of $CO_2$ absorption for post combustion capture in coal-fired power plants. Fuel 2009;88(12):2455–62.
[14] Ziaii S, Rochelle GT, Edgar TF. Dynamic modeling to minimize energy use for $CO_2$ capture in power plants by aqueous monoethanolamine. Ind Eng Chem Res 2009;48(13):6105–11.
[15] Lawal A, Wang M, Stephenson P, Yeung H. Dynamic Modeling and simulation of $CO_2$ chemical absorption process for coal-fired power plants. In: 10th International Symposium on Process Systems Engineering – PSE '09; 16–20 August 2009, Brazil; 2009.
[16] Kvamsdal HM, Rochelle GT. Effects of the temperature bulge in $CO_2$ absorption from flue gas by aqueous monoethanolamine. Ind Eng Chem Res 2008;47(3):867–75.
[17] Kvamsdal HM, Hetland J, Haugen G, Svendsen HF, Major F, Karstad V, Tjellander G. Maintaining a neutral water balance in a 450 MWe NGCC-CCS power system with post-combustion carbon dioxide capture aimed at offshore operation. Int J Greenhouse Gas Control; 2010. doi:10.1016/j.ijggc.2010.01.00.
[18] Doukelis A, Vorrias I, Grammelis P, Kakaras E, Whitehouse M, Riley G. Partial $O_2$-fired coal power plant with post-combustion $CO_2$ capture: a retrofitting option for $CO_2$ capture ready plants. Fuel 2009;88(12):2428–36.
[19] Onda K, Takeuchi H, Okumoto Y. Mass transfer coefficients between gas and liquid phases in packed columns. J Chem Eng Jpn 1968;1(1):56–62.
[20] Vaidya PD, Mahajani VV. Kinetics of the reaction of $CO_2$ with aqueous formulated solution containing monoethanolamine, N-methyl-2-pyrrolidone and diethylene glycol. Ind Eng Chem Res 2005;44(6):1868–73.
[21] Reid RC, Prausnitz JM, Sherwood TK. The properties of gases and liquids. 3rd ed. New York: McGraw-Hill; 1977.
[22] Oyenakan BA. Modeling of Strippers for $CO_2$ capture by Aqueous Amines. PhD Thesis. University of Texas at Austin; 2007.
[23] Dugas ER. Pilot plant study of carbon dioxide capture by aqueous monoethanolamine. MSE Thesis. University of Texas at Austin; 2006.